

## Surface Enrichment in Alcohol–Water Mixtures

G. Raina, G. U. Kulkarni, and C. N. R. Rao\*

Chemistry and Physics of Materials Unit, Jawaharlal Nehru Centre for Advanced Scientific Research, Jakkur P.O., Bangalore 560 064, India

Received: March 29, 2001; In Final Form: August 13, 2001

Molecular beams generated from the vapors above the surfaces of alcohol–water mixtures have been examined by mass spectrometry. The alcohols examined are methanol, ethanol, *n*-propanol, and *n*-butanol. The variation of the vapor-phase mole fraction of the alcohol, estimated from the cluster populations in the molecular beam, with the liquid mole fraction is found to be identical to that of the surface concentration of the alcohol in the liquid obtained from surface-tension measurements. The populations of the neat alcohol clusters, as distinct from those of alcohol–water clusters, also exhibit a comparable trend. Surface enrichment is considerably more pronounced in the case of *n*-butanol and *n*-propanol compared to that of ethanol.

### 1. Introduction

It is well-known that a fluid surface can cause the concentration of a component in a miscible mixture to be higher at the surface than in the bulk, a phenomenon commonly known as surface enrichment.<sup>1</sup> For a binary liquid mixture in contact with its vapor, each component may have its own concentration profile at the interfacial region depending on its volatility. This often results in a change in the surface tension of the solution relative to the pure components, the magnitude of the change depending on differences in the shape, size, and chemical nature of the molecules involved. Interesting trends have been observed in the compositional dependence of surface tension in alcohol–water mixtures.<sup>2,3</sup> While methanol produces a gradual decrease of the surface tension of aqueous solutions with an increase in concentration, ethanol and *n*-propanol produce more dramatic effects. Thus, in the case of *n*-propanol, the surface tension decreases sharply as the alcohol concentration is increased up to a composition beyond which it changes marginally. The phenomenon of surface enrichment by alcohol molecules in alcohol–water mixtures has intrigued many workers over the past few decades, much of the interest arising from the difficulty in predicting cluster nucleation rates from these liquid mixtures.<sup>4–9</sup> Schofield<sup>10</sup> and Guggenheim<sup>4</sup> employed the Gibbs adsorption equation and the knowledge of the partial molecular areas of ethanol and water at the surface to calculate the surface mole fraction of ethanol as a function of the bulk mole fraction. More recently, Laaksonen<sup>8</sup> has taken the surface tension of the alcohol–water mixture,  $\sigma(x_A)$ , to be proportional to the surface tensions of the pure substances multiplied by their volume fractions in the surface layer as given by the equation

$$\sigma(x_A) = \frac{(1 - x_A(s))v_W\sigma_W + x_A(s)v_A\sigma_A}{(1 - x_A(s))v_W + x_A(s)v_A} \quad (1)$$

Here,  $x_A$  and  $x_A(s)$  are the bulk and the surface mole fractions of the alcohol, respectively,  $v_W$  and  $v_A$  are the partial molecular volumes of water and alcohol, respectively, and  $\sigma_W$  and  $\sigma_A$  are the values of the surface tension of pure water and alcohol, respectively. The above equation was fitted to the experimental values of surface tension to obtain a relation between the surface and bulk mole fractions.

\* To whom correspondence should be addressed. Electronic mail: cnrrao@jncasr.ac.in.

Quantitative estimations of the concentration profiles of surface-active liquid mixtures are indeed difficult, although there has been some effort in this direction in the case of polymer blends.<sup>11–13</sup> With regard to miscible alcohol–water mixtures, there is a report on the ethanol–water system based on neutron reflectivity measurements.<sup>14</sup> The surface excess of ethanol estimated from the neutron study compares well with the values obtained using surface-tension data. The study, however, assumes different models for the distribution profiles of ethanol and water near the liquid surface. To obtain direct experimental evidence for surface enrichment, we have determined surface concentration profiles of ethanol–water and *n*-propanol–water mixtures over the entire compositional range by mass spectrometric analysis of the binary vapor in equilibrium with the liquid surface. For this purpose, we generated a cluster beam of the binary vapor swept off the surface of the alcohol–water liquid mixture, by injecting it into vacuum through a pulsed supersonic valve. The surface concentrations of the alcohols obtained in this manner show clear evidence of surface enrichment and exhibit interesting variations with the liquid composition. More importantly, they show one-to-one correspondence with the values estimated on the basis of surface tension and neutron data. We have employed this method to study the partially miscible *n*-butanol–water system as well. The rate at which the surface is enriched with an alcohol increases markedly with the increasing length of the hydrocarbon chain of the alcohol.

### 2. Experimental Section

Binary mixtures of the alcohols (HPLC grade, Aldrich) and water (quartz-distilled) were prepared with varying molar composition over the entire range at  $\sim 0.1$  intervals. To generate a molecular beam, 6 mL of the binary mixture was placed in a stainless steel cell connected to a pulsed supersonic valve (R. M. Jordan, USA) and was subjected to a helium back pressure of 2 atm from the top. The alcohol–water vapor was injected into a vacuum of  $10^{-7}$  Torr through a 0.5 mm orifice of the pulsed valve operating at 10 Hz and 4000 A. The details of this indigenous cluster apparatus are reported elsewhere.<sup>15</sup> Briefly, it consists of a cluster generation chamber, which is connected to a linear time-of-flight (TOF) mass spectrometer through a gate valve. A slit-skimmer assembly placed midway helps differential pumping of the two chambers. The molecular clusters were ionized using the 355 nm harmonic of a pulsed Nd:YAG laser (GCR-170) operating in the Q-switch mode (10

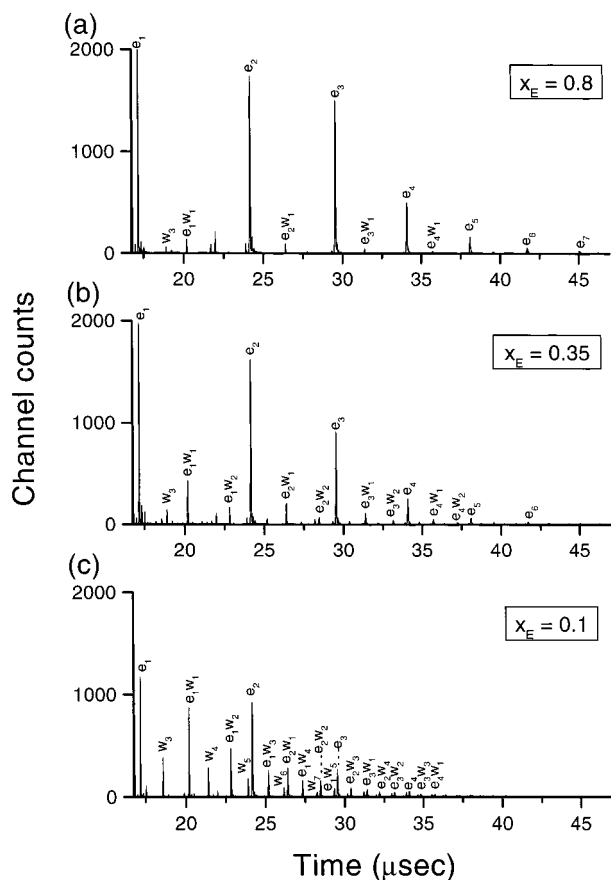


**Figure 1.** Time-of-flight mass spectra from ethanol–water mixtures for ethanol mole fraction in the liquid,  $x_E$ , of (a) 0.8, (b) 0.35, and (c) 0.1. The peaks are assigned to various protonated neat clusters of ethanol and water as well as mixed clusters.

Hz, 80 mJ/pulse). The extraction and acceleration voltages were held at 3000 and 1800 V, respectively. A microchannel plate detector (RMJ) was used for the detection of the ionized clusters. Mass spectra were collected using a multichannel scalar set to 16 000 channels with a dwell time of 20 ns/channel. Initial calibration was carried out using a variety of molecules such as acetone, water, and  $C_{60}$ . Mass resolution ( $T/2\Delta T$ ) of 800 was obtained in the linear TOF mode. For each binary mixture, the spectrum was collected under similar conditions after averaging the data in each channel over 5000 sweeps. Measurements were repeated at a few molar compositions to ascertain the reproducibility in the experiments (See Results and Discussion). To avoid residual contamination from a previous experiment, the pulse valve was pumped out each time before filling in the fresh vapor. A computer code developed in the laboratory has been used to analyze the mass spectra in terms of the abundance and the internal compositions of the various cluster species.

### 3. Results and Discussion

In Figure 1, we show the TOF mass spectra of ethanol–water (E–W) mixtures corresponding to the liquid mole fractions of ethanol,  $x_E$ , of 0.1, 0.35, and 0.8. The mass spectra of the last two compositions are dominated by neat ethanol clusters ( $E_nH^+$ ), mixed E–W clusters ( $E_nW_mH^+$ ) being associated with much smaller intensities. The  $E_nH^+$  clusters become prominent when  $x_E > 0.2$ , but their dominance persists even in the water-rich composition, as can be seen from Figure 1c. Clusters of water and the mixed species with higher water attachments are seen in the mass spectra of the water-rich compositions.

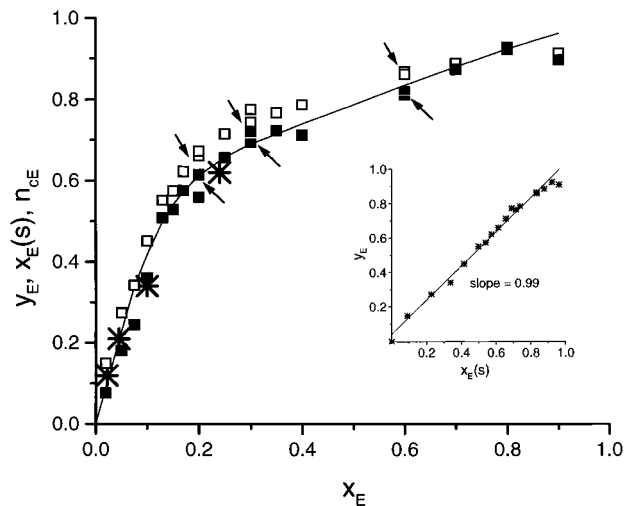


**Figure 2.** Variation in the mole fraction of ethanol in the vapor,  $y_E$  (□), and the relative population of neat ethanol clusters,  $n_{cE}$  (■), with the mole fraction of ethanol in liquid,  $x_E$ . The solid curve represents the surface mole fraction of ethanol,  $x_E(s)$ , taken from ref 8. The neutron values are also shown (\*). Arrows indicate the repeat experiments. The inset shows the variation of  $y_E$  with  $x_E(s)$ .

We could obtain the values of the vapor mole fraction of ethanol,  $y_E$ , by counting the number of ethanol molecules in the neat as well as the mixed cluster species. Thus,

$$y_E = \frac{\sum n}{\sum n + \sum m} \quad (2)$$

where  $n$  and  $m$  correspond to the number of ethanol and water molecules in a cluster; the summations are over all the cluster species both neat and mixed. In Figure 2, we show the variation of  $y_E$  with the liquid mole fraction of ethanol,  $x_E$ , in the ethanol–water mixtures. The data points of the repeat experiments at  $x_E$  of 0.2, 0.3, and 0.6 provide an average estimate of the experimental error ( $\pm 0.02$ ) in  $y_E$ . The mole fraction of ethanol in the vapor increases sharply reaching a value of  $\sim 0.6$  at  $x_E \approx 0.2$ , beyond which the increase in  $y_E$  is gradual. The variation of  $y_E$  with  $x_E$  in Figure 2 is a clear reflection of surface enrichment. We have plotted the values of surface concentration of ethanol,  $x_E(s)$ , reported by Laaksonen<sup>8</sup> against  $x_E$  in Figure 2. It is remarkable that the variation of  $x_E(s)$  with  $x_E$  is identical to that of  $y_E$ . Accordingly, the plot of  $y_E$  vs  $x_E(s)$  is linear with a slope of unity as shown in the inset of Figure 2. To compare our results quantitatively with those from neutron measurements,<sup>14</sup> we had to convert the surface excess values expressed in  $\text{mol cm}^{-2}$  in the literature to  $x_E(s)$  values. For this purpose, the surface layer was taken to be 5.5 Å thick (approximate length of ethanol molecule<sup>14,16</sup>), and the number of moles per cubic centimeter of ethanol in the surface layer was obtained by adding the surface excess of ethanol per cubic centimeter to the bulk concentration. A similar quantity was obtained for water by subtracting the surface excess from the bulk. These values were used to estimate  $x_E(s)$ . The final equation is as follows:

$$x_E(s) = \frac{\Gamma}{l}(x_W V_W + x_E V_E) + x_E \quad (3)$$

where  $\Gamma$  is the surface excess from neutron measurements,<sup>14</sup>  $l$  is the length of the ethanol molecule, and  $V_E$  and  $V_W$  stand for molar volumes of ethanol and water, respectively. In Figure 2, we have shown the  $x_E(s)$  values thus obtained from neutron data for compositions reported. As can be seen from the figure, the

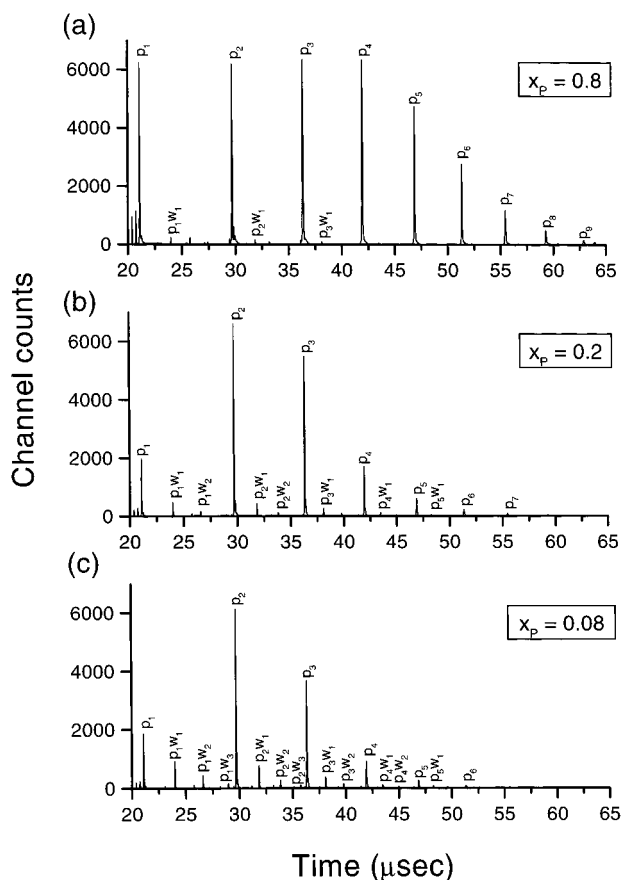


**Figure 3.** Time-of-flight mass spectra from *n*-propanol–water mixtures for propanol mole fraction in the liquid,  $x_p$ , of (a) 0.8, (b) 0.2, and (c) 0.08. The peaks are assigned to various protonated neat clusters of propanol and water as well as mixed clusters. The relative increase in the signal strength compared to Figure 1 is due to an additional set of deflection plates employed in the flight tube.

neutron values agree closely with our data. These results justify the use of the cluster beam for obtaining the compositional profiles of the surfaces of alcohol–water mixtures.

In Figure 2, we have also shown the variation of the relative population of neat ethanol clusters,  $n_{cE}$ , with  $x_E$ . The variation of  $n_{cE}$  with  $x_E$  parallels that of  $y_E$ , indicating that the major contribution to the mole fraction of ethanol in the vapor phase comes from the neat clusters of the alcohol. Below  $x_E \approx 0.2$ , however, the difference between  $y_E$  and  $n_{cE}$  becomes large indicating the presence of several mixed species in this concentration regime. Our results are consistent with the observations of Matsumoto et al.<sup>17</sup> who found no clusters characteristic of the aqueous medium for  $x_E \geq 0.2$ , the dominant species being ethanol clusters and their hydrates.

In Figure 3, we show the mass spectra from *n*-propanol–water (P–W) mixtures corresponding to the liquid mole fractions of propanol,  $x_p$ , of 0.08, 0.2, and 0.8. As in the case of ethanol, we observe that neat propanol clusters ( $P_nH^+$ ) dominate the spectra at all the compositions. Mixed cluster species ( $P_nW_mH^+$ ) containing a few water molecules ( $m \leq 3$ ) are present only in water-rich compositions. Figure 4 shows the variations of the experimental vapor mole fraction,  $y_p$ , and the surface mole fraction,  $x_p(s)$ , from the calculations of Laaksonen<sup>8</sup> with the liquid mole fraction,  $x_p$ . For  $x_p \leq 0.1$ , there is a steep rise in  $y_p$  to a value of  $\sim 0.85$ , the increase being rather gradual for  $x_p \geq 0.1$ . The agreement between the experimental vapor mole fractions,  $y_p$ , and the calculated values of  $x_p(s)$  is excellent in this system as well. The plot  $y_p$  vs  $x_p(s)$

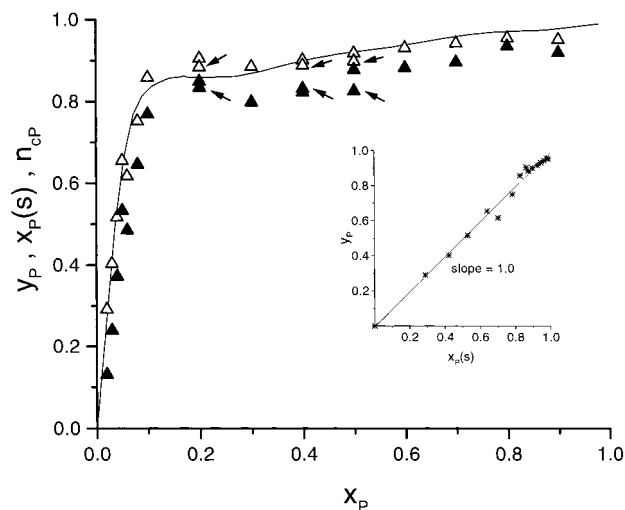


**Figure 4.** Variation in the mole fraction of propanol in the vapor,  $y_p$  ( $\Delta$ ), and the relative population of neat propanol clusters,  $n_{cP}$  ( $\blacktriangle$ ), with mole fraction of propanol in liquid,  $x_p$ . The solid curve represents the surface mole fraction of propanol,  $x_p(s)$ , taken from ref 8. Arrows indicate the repeat experiments. The inset shows the variation of  $y_p$  with  $x_p(s)$ .

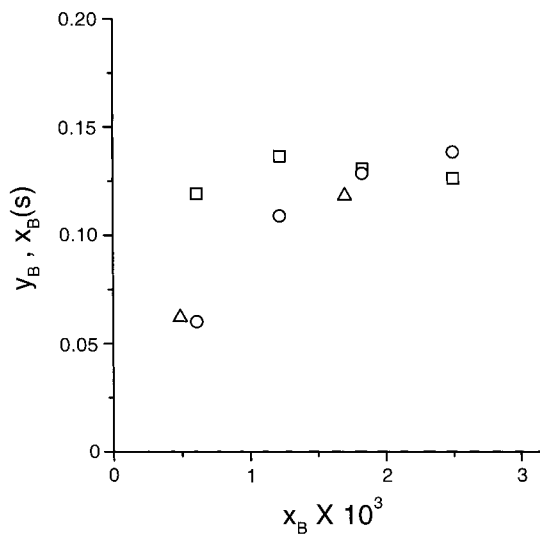


**Figure 5.** Variation in the mole fraction of butanol in the vapor,  $y_B$  ( $\square$ ), with mole fraction of butanol in liquid,  $x_B$ . Circles ( $\circ$ ) and triangles ( $\Delta$ ) represent the surface mole fraction of butanol,  $x_B(s)$ , from surface tension and neutron data, respectively (from ref 18).

is perfectly linear, with a slope of unity (see inset of Figure 4). The variation in the population of neat propanol clusters,  $n_{cP}$ , with  $x_p$  mimics that of  $y_p$ , similar to the situation observed in the case of the ethanol–water system.

Having established the reliability of the method to determine surface enrichment in miscible water–ethanol and water–propanol systems, we sought to examine the *n*-butanol–water system of which the miscibility is limited to a butanol mole fraction,  $x_B$ , of 0.02. In Figure 5, we show the variation of  $y_B$  with  $x_B$  along with  $x_B(s)$  values derived from surface tension data.<sup>18</sup> We are able to compare the present results with those from a neutron reflectivity study<sup>18</sup> performed in the miscible regime of this system (Figure 5). The surface excess values from the neutron study were converted to  $x_B(s)$  assuming the length of the *n*-butanol molecule to be  $7 \text{ \AA}$ .<sup>18</sup> We notice from Figure 5 that the  $y_B$  values lie close to the  $x_B(s)$  values from surface tension and neutron data, albeit the sensitivity of our method is lower at very low alcohol concentrations. Unlike in other

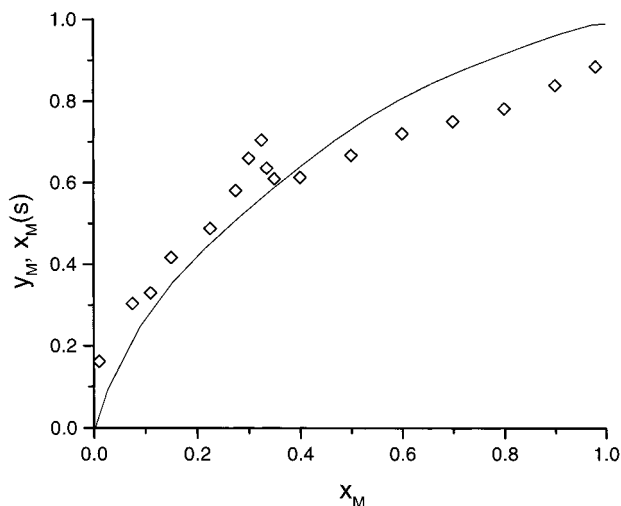


**Figure 6.** Variation in the mole fraction of methanol in the vapor,  $y_M$  ( $\diamond$ ), with mole fraction of methanol in liquid,  $x_M$ . The solid curve represents the surface mole fraction of methanol,  $x_M(s)$ , taken from ref 8.

alcohols, the surface enrichment in the butanol–water system is reached at an extremely low concentration of the alcohol ( $x_B \approx 0.0025$ ).

We have investigated the methanol–water system as well. Methanol being the smallest molecule in the series ( $\sim 4 \text{ \AA}$ ), one would expect a relatively poor surface enrichment in the methanol–water system. The plot in Figure 6 does indeed present such a scenario. Unlike in the case of higher alcohols, the mole fraction of methanol in the vapor,  $y_M$ , increases rather gradually with the increasing mole fraction of methanol,  $x_M$ , in the liquid. The agreement between our data and the Laaksonen's model is only moderately good. At low  $x_M$ , the experimental mole fraction,  $y_M$ , is overestimated in comparison to the value of the surface mole fraction,  $x_M(s)$ , while at high  $x_M$ ,  $y_M$  is somewhat underestimated. Unfortunately, because of the absence of literature data from neutron reflection, we are unable to compare our results. It appears that the molecular beam from the methanol–water system reveals a liquid surface which is barely different from the bulk and that the bulk thermodynamic properties may to some extent influence the nature of the species in the molecular beam.<sup>19,20</sup> Accordingly, the methanol–water system shows an anomaly at  $x_M \approx 0.3$ .

#### 4. Conclusions

In conclusion, we have demonstrated that the cluster beam produced from the binary vapor in equilibrium with the surface of an alcohol–water mixture can be used to obtain composition profiles of the surface. The method faithfully reflects the surface concentrations in the alcohol–water mixtures. Neat alcohol clusters dominate the cluster beam right from the dilute regime, implying that the surface of the liquid is mainly made up of a stratum of alcohol molecules, perhaps a monolayer thick. The degree of surface enrichment in the different alcohol–water systems can be compared in terms of the initial slopes of the plots of the vapor mole fraction,  $y_A$ , against the liquid mole fraction,  $x_A$  (Figures 2, 4–6). In Figure 7, we show variation of the slopes with the number of carbon atoms in the alcohol. With the increasing length of the alcohol molecule, the liquid surface is enriched at a faster rate. This is also evident from the inset in Figure 7, in which we show the variation of  $y_A$  with chain length for fixed values of  $x_A$ . In the case of the higher alcohols, once the surface is enriched at high  $x_A$ , the surface

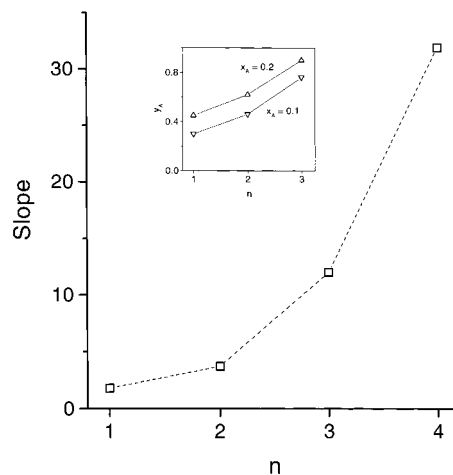


**Figure 7.** Slopes of the plots of  $y_A$  vs  $x_A$  for the various alcohol–water systems against the number of carbon atoms in the alcohol molecule,  $n$ , in the low-concentration regime prior to saturation of surface enrichment ( $\square$ ). The inset shows the variation of  $y_A$  with  $n$  for  $x_A = 0.1$  ( $\nabla$ ) and  $0.2$  ( $\triangle$ ).

composition hardly changes with the liquid composition (see Figures 2 and 4). It is also interesting that as the length of the alcohol molecule increases, the saturation of surface enrichment occurs at progressively lower concentrations of the alcohol in the liquid mixture. Thus, the saturation occurs at  $x_A$  of  $\sim 0.3$ ,  $0.2$ ,  $0.1$ , and  $0.0025$  for methanol, ethanol,  $n$ -propanol, and  $n$ -butanol systems, respectively. Accordingly, the surface activity of an alcohol molecule in an aqueous mixture increases with the increasing length of its hydrocarbon chain, eventually leading to partially miscible mixtures forming two layers.

#### References and Notes

- (1) Cahn, J. W. *J. Chem. Phys.* **1977**, *66*, 3667.
- (2) Myers, D. *Surfaces, Interfaces, and Colloids, Principles and Applications*; VCH: New York, 1991.
- (3) Ozawa, A.; Minamisawa, A. *Jpn. J. Appl. Phys.* **1977**, *36*, 2951.
- (4) Guggenheim, E. A. *Thermodynamics*; North-Holland: Amsterdam, 1967.
- (5) Zahoransky, R. A.; Peters, F. *J. Chem. Phys.* **1985**, *83*, 6425.
- (6) Wilemski, G. *J. Phys. Chem.* **1987**, *91*, 2492.
- (7) Schmitt, J. L.; Whitten, J.; Adams, G. W.; Zalabsky, R. A. *J. Chem. Phys.* **1990**, *92*, 3693.
- (8) Laaksonen, A. *J. Chem. Phys.* **1992**, *97*, 1983.
- (9) Viisanen, Y.; Strey, R.; Laaksonen, A.; Kulmala, M. *J. Chem. Phys.* **1994**, *100*, 6062.
- (10) Schofield, R. K.; Ridel, E. K. *Proc. R. Soc. London, Ser. A* **1925**, *109*, 60.
- (11) Penfold, J.; Thomas, R. K. *J. Phys.: Condens. Matter* **1990**, *2*, 1369.
- (12) Zhao, X.; Zhao, W.; Sokolov, J.; Rafailovich, M. H.; Schwarz, S. A.; Wilkens, B. J.; Jones, R. A. L.; Kramer, E. J. *Macromolecules* **1991**, *24*, 5991.
- (13) Roser, S. J.; Felici, R.; Eaglesham, A. *Langmuir* **1994**, *10*, 3853.
- (14) Li, Z. X.; Lu, J. R.; Styrkas, D. A.; Thomas, R. K.; Rennie, A. R.; Penfold, J. *Mol. Phys.* **1993**, *80*, 925.
- (15) Raina, G.; Kulkarni, G. U.; Yadav, R. T.; Ramamurthy, V. S.; Rao, C. N. R. *Proc.—Indian Acad. Sci., Chem. Sci.* **2000**, *112*, 83.
- (16) If, as an upper limit, the length of the molecule is assumed to be  $7 \text{ \AA}$ , the value of  $x_E(s)$  changes to some extent. For example, at  $x_E$  of  $0.045$ ,  $x_E(s)$  came out to be  $0.18$  compared to  $0.21$  for  $5.5 \text{ \AA}$  length.
- (17) Matsumoto, M.; Nishi, N.; Furusawa, T.; Saita, M.; Takamuku, T.; Yamagami, M.; Yamaguchi, T. *Bull. Chem. Soc. Jpn.* **1995**, *68*, 1775.
- (18) Li, Z. X.; Lu, J. R.; Thomas, R. K.; Rennie, A. R.; Penfold, J. *J. Chem. Soc., Faraday Trans.* **1996**, *92*, 565.
- (19) Raina, G.; Kulkarni, G. U. *Chem. Phys. Lett.* **2001**, *337*, 269.
- (20) Takamuku, T.; Yamaguchi, T.; Asato, M.; Matsumoto, M.; Nishi, N. *Z. Naturforsch.* **2000**, *55A*, 513.